Name: Pek Chuen Jye

Supervisor: Dr. Wolfram Just

Project title and Module Code: Analytical and numerical analysis of the Burgers' equation (MTHM038)

Analytical and numerical analysis of the Burgers' equation

Abstract. The project aims to perform analytical and numerical analysis on partial differential equations. In particular, the project will consider the Burger's equation. The project will aim to solve for analytical solutions of the Burger's equation and then comparing them with the numerically simulated solutions. The analytical analysis will examine the effects of the diffusive coefficient (viscosity) and its impact on particular types of solutions. The numerical analysis will focus on the stability of the discretisation scheme.

1 Introduction

The Burgers' equation is a quasilinear parabolic partial differential equation (PDE) which was initially proposed by Bateman during 1915 as a method study shock profiles. It was later applied to study turbulence by Burgers in 1940s; hence the name Burgers equation. Then, Cole and Hopf each independently found exact solutions to the equation. The transformation method is recognized as Cole-Hopf transformation where the quasilinear PDE is transformed into a linear diffusion equation, also known as the heat equation. There exist many solutions for the Burgers equation. For example, there are 35 solutions surveyed by Benton et al.[4].

The general form of the equation also known as viscous Burgers' equation is as follows:

$$u_t + uu_x = \epsilon uu_x. \tag{1.1}$$

Alternatively it can be written as [2]:

$$\underbrace{\frac{\partial u}{\partial t}}_{Unsteady\ term} + \underbrace{u\frac{\partial u}{\partial x}}_{Convective\ term} = \underbrace{\nu\frac{\partial^2 u}{\partial x^2}}_{Viscous\ term},$$

or

$$u_t + \left(\frac{1}{2}u^2\right)_x \#(1.2)$$

As a result, it is a subject of interest when studying physical properties such as fluid motions governed by nonlinear fluid equations,

for the momentum equations in fluid mechanics

Other attempts have also been made to solve (1.1) analytically. For example,Wazwaz used the tanh-coth method to examine solutions for a single front wave (kink) solution and the traveling wave solution as well using the Coth-Hopf transformation to examine multiple front solutions of the coupled Burgers equations [21]. By implementing a modified tanh-coth method, Wazzan solved the Korteweg-de Vries and Korteweg-de Vries–Burgers' equation [22]. To modify the one-dimensional burgers' equation, Momani substitute the Caputo fractional derivative [19].

Gomez solved the result for fractional burgers equation through fractional complex transform [11].

Another aspect of the Burgers equation is often being used to analyse properties of numerical schemes due to having analytical solutions. In 1999, Kutluay et al. [16] compared the analytical solution of the viscous Burgers equation with solutions approximated via explicit finite difference scheme and exact-explicit finite difference scheme. In 2006, Kadalbajoo et al. [14] approximate the solutions using a Crank-Nicolson finite difference scheme onto the linearized Burgers equation. Inan et al. [12]modified the finite difference schemes to use implicit and fully implicit exponential finite difference schemes.

A thorough review into literature of the Burgers' equation can found in [5] which consist of research from1915 until 2017.

For the rest of report, the content is structured as follows. In section 2, an example on how the Burgers equation resembles another model is shown. In section 3, the analytical solutions of the Burgers equation will be discussed, first in its viscous form and then its inviscid form. In section 4, a brief review of the background for numerical methods is first given, followed by discussion on how to assess the numerical schemes. The numerical schemes implemented are then provided. In section 5, numerical results are given where certain *initial value problems* are considered. In section 6, the relationship between the viscous and inviscid forms of the Burgers' equation will discussed via the *vanishing viscosity approach*.

2 Analog of the Burgers' equation

One of the key reasons that Burgers' equation is widely investigated is due to how it can be represented as an easier counterpart for more complicated models. By using it as a toy model, one could study the intrinsic properties of more arduous problems at a lesser complexity.

2.1 Euler equation

For example, the Euler equations in 1D are:

$$\begin{cases} \dfrac{\partial \rho}{\partial t} + \dfrac{\partial}{\partial x}(\rho u) = 0 \\ \dfrac{\partial}{\partial t}(\rho u) + \dfrac{\partial}{\partial x}(\rho u u + P) = 0 \\ \dfrac{\partial}{\partial t}(\dfrac{1}{2}\rho u^2 + \rho e) + \dfrac{\partial}{\partial x}((\rho u^2 + pe + P)u) = 0 \end{cases}$$

First, reformulate the equation of motion:

$$\frac{\partial}{\partial t}(\rho u) + \frac{\partial}{\partial x}(\rho u u + P) = 0$$

$$u\frac{\partial \rho}{\partial t} + u\frac{\partial}{\partial x}(\rho u) + \rho\frac{\partial u}{\partial t} + (\rho u)\frac{\partial u}{\partial x} + \frac{\partial P}{\partial x} = 0$$

$$\rho\frac{\partial u}{\partial t} + (\rho u)\frac{\partial u}{\partial x} + \frac{\partial P}{\partial x} = 0$$

and then neglect the pressure gradients $\frac{\partial P}{\partial x} = 0$, resulting in the inviscid Burgers' equation:

$$\frac{\partial u}{\partial t} + u\frac{\partial u}{\partial x} = 0.$$

In the next section, both viscous and inviscid forms of the equation will be examined analytically.

3 Analytical solution of the Burgers Equation

3.1 Viscous Form

The following initial value problem of (1.1) will be examined.

$$\begin{cases} u_t + uu_x = \epsilon u_{xx}, & x \in \mathbb{R}, t > 0, \\ u(x,0) = f(x), & x \in \mathbb{R} \end{cases} \tag{3.1.1}$$

Exact solution

The equation (1.1) can be solved exactly by transforming its non-linear form into the linear diffusion equation. The transformation method is called the Cole-Hopf method that utilizes the nonlinear transformation

$$u(x,t) = -2\epsilon\frac{\theta_x}{\theta} \tag{3.1.2a}$$

which has an equivalent form of

$$u(x,t) = -2\epsilon\frac{\partial}{\partial x}(\log\theta) \tag{3.1.2b}$$

where $\theta(x,t)$ is a solution to the heat equation. Lastly, by rearranging (3.1.2b) and taking its integration gives

$$\theta(x,t) = \exp\left(-\frac{1}{2\epsilon}\int_0^x u(\mathrm{H},t)\,d\mathrm{H}\right)$$

(3.1.2a) can be verified as a solution which satisfies equation (1.1) by differentiating accordingly. Thus, the transformation reduces (3.1.1) into

$$\begin{cases} \theta_t - \epsilon\theta_{xx} = 0, & x \in \mathbb{R}, t > 0, \\ \theta(x,0) = \exp\left(-\frac{1}{2\epsilon}\int_0^x u(\mathrm{H},0)\,d\mathrm{H}\right), & x \in \mathbb{R} \end{cases} \tag{3.1.3}$$

To solve (3.1.3), recall that the homogeneuous initial value problem of heat equation`

$$\begin{cases} \Theta_\mathrm{t} - a\Theta_{\mathrm{xx}} = 0 \\ \Theta(\mathrm{x},0) = g \end{cases}$$

has the solution of the form

$$\Theta(x,t) = \int_{\mathbb{R}} \phi(x-y,t)g(y)dy, \qquad x \in \mathbb{R}, t > 0$$

where the fundamental solution ϕ $s(x, t > 0) = \frac{1}{(4a\pi t)^{\frac{n}{2}}} \exp - \frac{|x|^2}{4at}$. Hence, by comparison the solution of (3.1.3) can be deduced as

$$\theta(x,t) = \frac{1}{(4\epsilon\pi t)^{\frac{n}{2}}} \int_{\mathbb{R}} \left(\exp - \frac{|x-\eta|^2}{4\epsilon t} \exp\left(-\frac{1}{2\epsilon} \int_0^x u(\mathrm{H}, 0)\, d\mathrm{H} \right) \right) \mathrm{d}\eta \,.\#(3.1.4)$$

The exact integral solution of (3.1.1) can then be obtained by substituting (3.1.4) into (3.1.2a) which in turn gives

$$u(x,t) = \frac{\int_{\mathbb{R}} (\exp - \frac{|x-\eta|^2}{4\epsilon t} \exp\left(-\frac{1}{2\epsilon} \int_0^x u(\mathrm{H},0)\, d\mathrm{H} \right) u(\eta,0)) d\eta}{\int_{\mathbb{R}} \exp - \frac{|x-\eta|^2}{4\epsilon t} \exp\left(-\frac{1}{2\epsilon} \int_0^x u(\mathrm{H},0)\, d\mathrm{H} \right) \mathrm{d}\eta} \#(3.1.5)$$

as seen in [6,7, 8].

Traveling wave solutions. As the Burgers equation can be used to study shock profiles, another solution in the form of

$$u(x,t) = u(\varepsilon), \qquad \varepsilon = x - Ut \ \#(3.1.5)$$

can be used to determine the relationship between nonlinear steepening and viscosity. Such a solution is often referred to as a traveling wave solution. Here, U represents the wave speed and $u(\varepsilon)$ represents the wave form. Substituting (3.1.5) back into (1.1) returns the following form

$$-Uu'(\varepsilon) + uu'(\varepsilon) - \nu u''(\varepsilon) = 0.$$

Then, by taking its integration

$$-Uu(\varepsilon) + \frac{1}{2}u^2 - \nu u'(\varepsilon) = A,$$

where A is a constant of integration, which can be rearranged as

$$u'(\varepsilon) = \frac{1}{2\nu}(u^2 - 2Uu - 2A) = 0.$$

Hence, U and A can be determined via the two roots of the quadratic equation where

$$u_{1,2} = U \pm \sqrt{U^2 + 2A}, \qquad u_1 > u_2$$

and

$$U = \frac{1}{2}(u_1 + u_2), \qquad A = -\frac{1}{2}u_1 u_2.$$

Writing the equation in terms of its roots and then by partial integrations gives

$$\frac{\varepsilon}{2\nu} = -\int \frac{du}{d(u_1 - u)(u - u_2)} = \frac{1}{u_2 - u_1} \log |\frac{u - u_2}{u - u_1}|$$

Next, by multiplying both sides with -1,

$$\frac{\varepsilon}{2\nu}(u_1-u_2)=\log\left|\frac{u-u_1}{u-u_2}\right|=\log\frac{|(-1)(u-u_1)|}{|u-u_2|}=\log(\frac{u_1-u}{u-u_2})$$

Finally, the solution can be obtained in form of

$$u(\varepsilon)=\frac{u_1+u_2\exp[(\frac{\varepsilon}{2\nu})(u_1-u_2)]}{1+\exp[(\frac{\varepsilon}{2\nu})(u_1-u_2)]}$$

which can be rewritten as [7]:

$$u(\varepsilon)=\frac{1}{2}(u_1+u_2)+\frac{u_1+u_2\exp\left[\left(\frac{\varepsilon}{2\nu}\right)(u_1-u_2)\right]}{1+\exp\left[\left(\frac{\varepsilon}{2\nu}\right)(u_1-u_2)\right]}-\frac{1}{2}(u_1+u_2)$$

$$=U-\frac{1}{2}(u_1-u_2)\tanh\left[\left(\frac{\varepsilon}{4\nu}\right)(u_1-u_2)\right].\#(3.1.6)$$

The wave profile exhibits certain properties. As $\xi\to\pm\infty$, $u(\xi)$ tends asymptotically to the quadratic roots u_2 and u_1 respectively, which can be observed in figure 1. Furthermore, the value of the viscosity ϵ affects the shape of the wave form significantly. Indeed, as the viscosity coefficient becomes smaller, the wave form begins to distort. Hence, viscosity is required in order to prevent wave form from breaking. Similarly, one can also observe that with large viscosity coefficient, the wave form is eventually flattened into a horizontal straight line; the diffusion effect is strong to the point where no waves can be formed.

Figure 1: Traveling wave solution with different viscosity values ($u_1=0.75, u_2=0.05$)

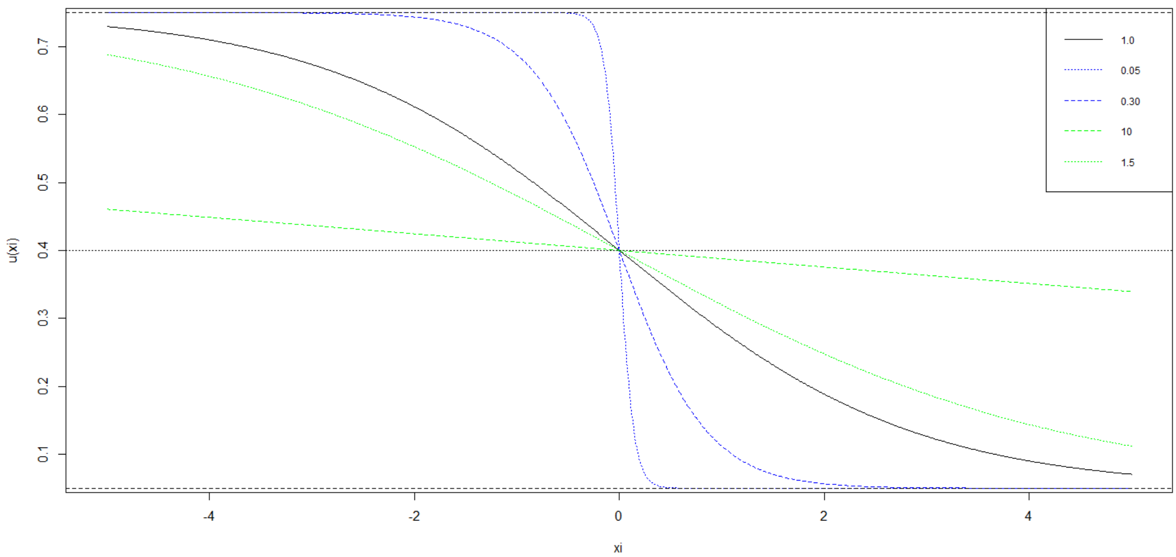

3.2 Inviscid

When the diffusive term is neglected $\epsilon = 0$, the equation becomes a hyperbolic equation

$$u_t + uu_x = 0. \tag{3.2.1}$$

which has a conservation form

$$u_t + (F(u(x,t)))_x = 0$$

where $F(u) = \frac{1}{2}u^2$is a flux function.

Method of Characteristics. The equation (3.2.1) can be solved via method of characteristics which essentially reduces the hyperbolic PDE into a system of uncoupled first order ODEs, giving a general solution F

$$F(c_1, c_2) = 0$$

where F is an arbitrary differentiable function with constants c_1 and c_2. Here, the characteristic equations are

$$\frac{dx}{u} = \frac{dt}{1} = \frac{du}{0} \tag{3.2.2}$$

This suggests that u is a constant. Rearranging (3.2.2), the following ODE can be obtained

$$\frac{dx}{dt} = u = c_1$$

which integrates to

$$x = c_1 t + c_2 = ut + c_2. \tag{3.2.3}$$

Therefore $c_2 = x - ut$, resulting in the general implicit solution

$$u(x,t) = F(x - ut).$$

Furthermore, (3.2.3) implies that the solution is constant along the characteristic curves defined by

$$x(t) = x_0 + ut$$

Hence, the general implicit solution associated with the initial condition $u(x,0) = u_0(x) = F(x)$ is

$$u(x,t) = u_0(x - ut). \#(3.2.4)$$

The characteristics are then described by

$$x(t) = x(0) + ut.$$

<u>Example 1:</u>

Consider the following piecewise constant initial condition which is also known as a *Riemann problem*:

$$u(x,0)=\begin{cases}-a & \text{if } x<0\\ a & \text{if } x\geq 0\end{cases}, \qquad \#(3.2.5)$$

For starters, consider the case when $a=1$. The resulting characteristic lines projected onto the $(x-t)$ plane resemble a V shape as seen in figure 2 below. When $x(0)<0$, the lines are governed by $t=-(x(t)-x(0))$ with solution $u(x,t)=-1$. Similarly, when $x(0)\geq 0$, the lines are governed by $t=(x(t)-x(0))$ with solution $u(x,t)=1$. However, in areas beyond the V shape there exist no characteristic lines, a discontinuity has occurred.. This implies that the initial data has no *classical* solution there; i.e. initial value problem does not in general have a smooth solution existing for all times $t>0$. The example highlights that none smooth solutions exist for initial value problems or alternatively, smooth solutions only exist within some finite time interval.

Figure 2: Characteristic lines of u(x,0) when $a=1$

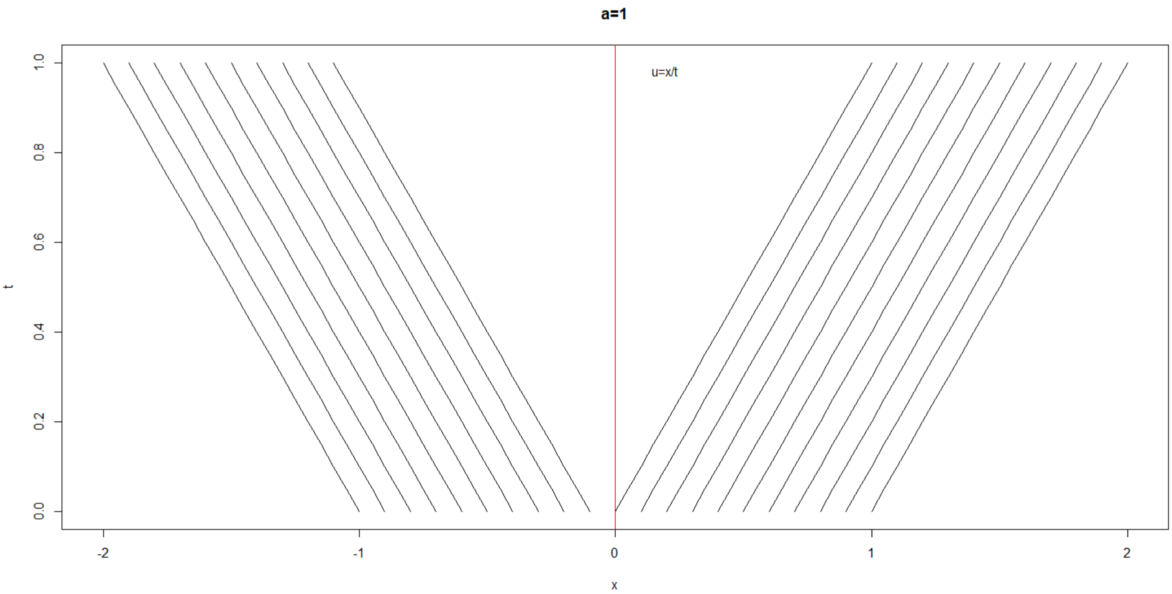

As the characteristic lines are essentially discretized lines projected from the x-axis, one could imagine with smaller a and more discretized $x(0)$ values that the characteristic lines would be steeper and have covered more regions, suggesting perhaps some compromise can be made to construct an acceptable solution. Hence, there is the need to allow for *weak* solutions. A weak solution is essentially an integral solution to the initial value problem to (3.2.1) which does not require the smoothness of a classical solution. For detailed explanations readers may refer to [7,8,17] but the main idea is as follows:

1. Consider u as a smooth solution and also introducing another smooth function $v:\mathbb{R}\times[0,\infty)$ which is bounded within a compact set, i.e. its value is zero when considering beyond boundaries of set A. This is often referred to as a test function.
2. Multiply the test function v onto equation (3.2.1) and then apply integration by parts over the intervals $-\infty<x<\infty$ and $0\leq t<\infty$.

3. The resulting equality gives
    a. $\int_0^\infty \int_{-\infty}^\infty \left(uv_t + \frac{1}{2}u^2 v_x\right) dxdt + \int_0^\infty u(x,0)v(x,0)dx = 0$ #(3.2.6)
4. Therefore, $u(x,t)$ is a weak solution of (3.2.1) if (3.2.6) holds.
5. An informal way to understand why this is equality leads to a less rigorous solution is to consider that the equation now involves fewer derivatives on u, and hence requiring less smoothness.

An immediate consequence of allowing weak solutions is solutions may not always be unique. To ensure uniqueness of solutions certain conditions will have to be imposed, namely the Rankine-Hugoniot jump condition and the Lax entropy criterion.

Rankine-Hugoniot jump condition. When the weak solution u is discontinuous across a curve $x(t) = (x - ut)$ on the $(x - t)$ plane and yet remain smooth on either side of the curve, u then must satisfy the jump condition. This can be derived from the Riemann problem where a shock occurs under the conservation law with a piecewise constant initial data [18]. The condition for the scalar equation (3.2.1) then returns the speed of propagation of the shock as

$$s = \frac{f(u_R) - f(u_L)}{u_R - u_L} = \frac{1}{2}(u_L + u_R) \#(3.2.7)$$

where u_L and u_R are the smooth solutions beside the discontinuous curve.

Lax entropy criterion. The entropy criterion is based on the second law of thermodynamics where entropy increases across a shock. Essentially, this means that the wave speed right before a shock is greater than the wave speed after the shock. This can be formulated as

$$a(u_l) > U > a(u_r)$$

where $a(u) = u$ for inviscid Burgers equation. Hence, a shock is when a discontinuity satisfying both the RH jump condition and the Lax entropy criterion on its curve of discontinuity.

Another type of discontinuity that exists is the rarefaction wave. Its solution can be determined via ansatz [15]

$$u(x,t) = r\left(\frac{x}{t}\right), \qquad -t \le \frac{x}{t} < t$$

where r is a differentiable function. By substitution into (3.2.1), the solution is then obtained as

$$r\left(\frac{x}{t}\right) = \frac{x}{t}, \qquad -t \le \frac{x}{t} < t.$$

Therefore, two possible solutions are

$$u_1(x,t) = \begin{cases} -1 & \text{if } x < 0 \\ 1 & \text{if } x \ge 0 \end{cases}$$

$$u_2(x,t) = \begin{cases} -1 & \text{if } x < -t \\ \frac{x}{t} & \text{if } -t \le x < t \\ 1 & \text{if } x \ge t \end{cases}$$

Both cases meet the jump condition but only $u_2(x,t)$ satisfies the entropy condition. Hence, the unique entropy solution to the initial value problem (3.2.5) is u_2, where the empty interval is now filled with new information. The next example will illustrate a shock occurring. Consider the initial value problem (3.2.5) again, but with $a = -1$.

Figure 3: Characteristic lines of u(x,0) when $a = -1$

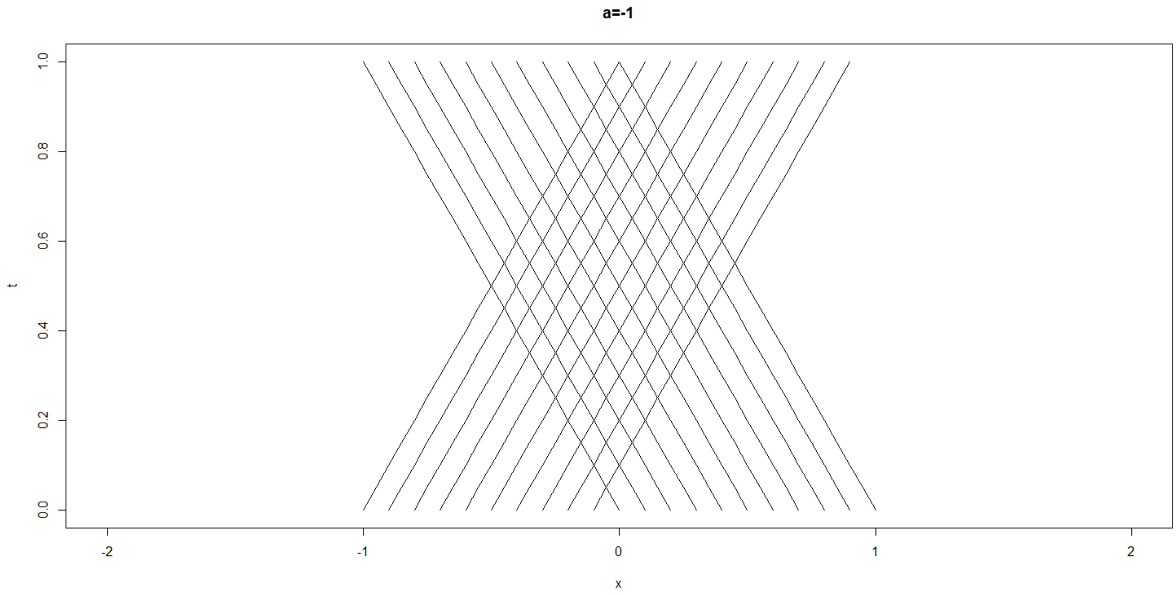

As expected when inverting the signs of a, the lines project to opposite directions from before. When $x(0) \geq 0$, the lines are governed by $t = -(x(t) - x(0))$ with solution $u(x,t) = -1$. Similarly, when $x(0) < 0$, the lines are governed by $t = (x(t) - x(0))$ with solution $u(x,t) = 1$. The key difference is that the lines now intersect. This means the solution have become multi-valued and are in contradiction; negative and positive lines produce the same solutions.

Breaking time. To examine the shock further, one could determine when the intersection of the characteristic lines occurs. This is called the breaking time and formulated as

$$\tau = -\frac{1}{\min \frac{\partial u(x,0)}{\partial x}} . \#(3.2.8)$$

Breaking time can be deduced from a number of ways, such as i) implicit function theorem applied to the implicit solution (3.2.4) and ii) using the mean value theorem onto intersection point of two characteristic lines to solve for τ.

Interestingly, the breaking time $\tau = 0$ in this scenario and indeed, it appears the initial value problem (3.2.1) with $a = -1$ is a static shock; the characteristic lines immediately collide. There remains the solution which is a max entropy solution

$$u(x,t) = \begin{cases} 1 & \text{if } x < 0 \\ -1 & \text{if } x \geq 0 \end{cases}$$

which indeed satisfies both the jump and entropy condition.

To summarize, the initial value problem of (3.2.1) was solved via the Method of Characteristics. Then the characteristic lines are projected onto the $(x - t)$ plane to obtain qualitative information of the solution. Lastly, the Rangine-Hugoniot jump condition and Lax entropy condition were imposed to ensure uniqueness of the solution. Furthermore, shock propagation is not always possible as seen from before when shock speed $s = 0$.

Note that despite having the method of characteristics, the hyperbolic equation (3.2.1) usually cannot be solved analytically. Hence, numerical methods are required to approximate the solution $u(x, t)$. This will be discussed in Section 4.

4 Numerical analysis

4.1 Background

There are a numerous ways of solving quasilinear PDEs numerically, such as finite difference, finite element, finite volume and spectral methods. In this report, only finite difference methods are implemented. Some common notations used for the numerical methods are first mentioned here.

- $\Delta x :=$ Interval of the step taken in the spatial direction
- $\Delta t :=$ Interval of the time step
- $u_{i,j} :=$ Estimated solution of the Burgers$'$equation at spatial point i and time j
- $\theta_{i,j} :=$
  Estimated solution of the transformed linear Burgers equation at spatial point i and time j
- $N :=$ The total number of steps(iterations)in spatial space $= \frac{1}{\Delta x}$
- $M :=$ The total number of steps(iterations)in time $= \frac{1}{\Delta t}$
- $T :=$ The final time $= M\Delta t$

4.1.1 Taylor series

Before discussing the different numerical schemes in greater details, a fundamental concept will be briefly reminded, namely the Taylor series. Consider an arbitrary differentiable function $f(x)$ and its Taylor expansion

$$f(x + \Delta x) = f(x) + \Delta x \frac{\partial f}{\partial x} + \frac{\Delta x^2}{2!}\frac{\partial^2 f}{\partial x^2} + \cdots + \frac{\Delta x^n}{n!}\frac{\partial^n f}{\partial x^n} + \cdots \#(4.1.1)$$

where the number of terms n is referred to as order of n. A series with order of n will then have errors determined by its omitted $n + 1$ terms onwards. In particular, the dominating error will be the Δx^{n+1} term which is referred to as the truncation error and denoted as

$$O(x^{n+1}).$$

Note that the truncation error does not mean the exact size of the truncation error. Instead, it gives an expectation on how it should behave as $\Delta x \to 0$.

4.1.2 Finite Difference approximations

Finite difference approximation is an approximation of a derivative by discretizing the dependent variables onto finite points. By doing so, the derivatives can then be replaced as algebraic equations and thus, reducing the need to directly solve complicated calculus problems.

From (4.1.1), by rearranging in terms of the first derivative and then only choosing up to the order $n = 1$, one could obtain the following difference equation

$$\frac{\partial f}{\partial x} = \frac{f(x + \Delta x) - f(x)}{\Delta x} + O(\Delta x)$$

which is referred to as the *forward difference*. Similarly, one could obtain the *backward difference* by using a backward Taylor expansion in (4.1.1) i.e. $f(x + (-\Delta x))$ which returns

$$\frac{\partial f}{\partial x} = \frac{f(x) - f(x - \Delta x)}{\Delta x} + O(\Delta x).$$

Lastly, by subtracting the backward difference from the forward differences, one can then obtain the *central difference*

$$\frac{\partial f}{\partial x} = \frac{f(x + \Delta x) - f(x - \Delta x)}{2\Delta x} + O(\Delta x^2).$$

As the derivations are mostly similar in nature, the remaining difference equations involved are stated without proof.

$Second\ derivative\ forward\ difference$:

$$\frac{\partial^2 f}{\partial x^2} = \frac{f(x + 2\Delta x) - 2f(x + \Delta x) + f(x)}{\Delta x^2} + O(\Delta x)$$

$Second\ derivative\ backward\ difference$:

$$\frac{\partial^2 f}{\partial x^2} = \frac{f(x - 2\Delta x) - 2f(x - \Delta x) + f(x)}{\Delta x^2} + O(\Delta x)$$

$Second\ derivative\ central\ difference$:

$$\frac{\partial^2 f}{\partial x^2} = \frac{f(x + \Delta x) - 2f(x) + f(x - \Delta x)}{\Delta x^2} + O(\Delta x^2)$$

An immediate observation is that both central differences provide a more accurate approximation as compared to their counterparts.

4.1.3 Assessing the approximations

As the numerical methods are approximations of the solutions, it crucial to understand the quality and properties of these methods and their estimations, i.e. accuracy and stability.

Accuracy. To determine how accurate the approximations are, one could use the difference between the exact and estimated values. One way of doing so is by computing the norms of the error. First, recall that the for $k = 1 \dots n$, norm of $|| \cdot ||_p$ for a real number p is defined as

$$||x||_p := \left(\sum_{k=1}^{n} |x_k|^p \right)^{\frac{1}{p}}$$

and in particular for $p = \infty$,

$$||x||_\infty := \max_{1\le k\le n} |x_k|.$$

Next, introduce the error metric as $error_k = x_k^{exact} - x_k^{estimate}$. Then, by treating it as mesh function using the Trapezoidal integration formula, the error can be computed as

$$||error||_p = \left(\frac{1}{N}\sum_{k=1}^{n} |error_k|^p\right)^{\frac{1}{p}}.$$

Specifically, the norm with $p = 2$

$$||error||_2 = \left(\frac{1}{N}\sum_{k=1}^{n} |error_k|^2\right)^{\frac{1}{2}} \#(4.1.2a)$$

and $p = \infty$

$$||error||_\infty := \max_{1\le k\le n} |error_k| \#(4.1.2b)$$

will be used to assess the accuracy of the approximations. Note that these errors are step size dependence due to the scaling of $\frac{1}{N}$.

Stability. The assessment is to measure the discrepancies from errors introduced by computations. For example, computers can only compute up till finite decimal points. Thus, round-off errors will be present. Here, the *Von Neumann method*, also known as *Fourier stability analysis*, will be used to determine stability criteria for the numerical methods implemented. For the detailed explanation, readers are referred to [9] but the main idea is to

1 Assume that the distribution of errors is represented by a Fourier series.
2 Making use of *Euler's* formula, the amplification factor G can be obtained.
3 From G, it can be further simplified to determine a stability criteria.

Note that this method is applicable for linear problems only. Hence when analysing the viscous equation (1.1), the Cole-Hopf transformation must be used.

4.1.4 Numerical schemes

Forward-Time Central-Space (FTCS). The FTCS explicit scheme, as its name suggests, is a first order scheme obtained from the combination of forward difference in the time derivative and a central difference in the spatial derivative. The following equations are based on the transformed linear equation as seen in [16]

$$\theta_{i,j+1} = (1-2r)\theta_{i,j} + 2r\theta_{i+1,j}, \qquad i = 0$$

$$\theta_{i,j+1} = r\theta_{i-1,j} + (1-2r)\theta_{i,j} + r\theta_{i+1,j}, \qquad i = 1{:}\,N-1$$

$$\theta_{i,j+1} = 2r\theta_{i-1,j} + (1-2r)\theta_{i,j}, \qquad i = N$$

where $r = k\epsilon/h^2$, k is the time step. A truncation error of $O(k) + O(h^2)$ can be expected. The final solution can then be obtained via the following conversion

$$u(x_i, t_j) = -\frac{\epsilon}{h}\left(\frac{\theta_{i+1,j} - \theta_{i-1,j}}{\theta_{i,j}}\right)$$

along with the stability requirements of

$$2\epsilon\frac{\Delta t}{\Delta x^2} \leq 1.$$

Implicit Crank Nicolson finite difference. The Crank Nicolson scheme is a second order in time scheme that can obtained from a central difference on the time derivative with half time steps, $t_j + \frac{1}{2}\Delta t$; and for the spatial derivative, the average between two points. The approximation are computed as seen in [14]

$$-r\theta_{i+1,j+1} + (1+r)\theta_{i,j+1} = r\theta_{i+1,j} + (1-r)\theta_{i,j}, \qquad i = 0$$

$$-\frac{r}{2}\theta_{i+1,j+1} + (1+r)\theta_{i,j+1} - \frac{r}{2}\theta_{(i-1,j+1)} = \frac{r}{2}\theta_{i+1,j} + (1-r)\theta_{i,j} + \frac{r}{2}\theta_{i-1,j}, \qquad i = 1{:}\,N-1$$

$$(1+r)\theta_{i,j+1} - r\theta_{(i-1,j+1)} = r\theta_{i-1,j} + (1-r)\theta_{i,j}, \qquad i = N$$

where $r = \Delta t\epsilon/h^2$. The final solution is also computed by #(5.1.5). Notice that a tridiagonal matrix was involved at each time step and the *Thomas Algorithm* was implemented to compute it.

By the Von Neumann stability, the implicit Crank Nicolson is unconditionally stable with a truncation error of $O(\Delta t^2 + \Delta x^2)$. This means that larger time steps can be taken without comprising the stability.

Lax method. By expanding a Taylor series of the conservative form of the Burgers equation (1.2), the following can be obtained via central differences and averaging the first term [2]

$$u_{j,n+1} = \frac{u_{j+1,n} + u_{j-1,n}}{2} - \frac{\Delta t}{\Delta x}\frac{F_{j+1,n} - F_{j-1,n}}{2}$$

where $F_{j,n} = \frac{u_{j,n}^2}{2}$ along with the stability requirement of

$$\left|\frac{\Delta t}{\Delta x}u_{\max}\right| \leq 1.$$

Lax-Wendroff. As an improvement to the first order Lax-method, the Lax-Wendroff scheme is second order and obtained by evaluated u at half time steps and half spatial direction

$$u_{j,n+1} = u_{j,n} - \frac{\Delta t}{\Delta x}\frac{F_{j+1,n} - F_{j-1,n}}{2} + \frac{1}{2}\left(\frac{\Delta t}{\Delta x}\right)^2 [A_{j+\frac{1}{2},n}(F_{j+1,n} - F_{j,n}) - A_{j-\frac{1}{2},n}(F_{j,n} - F_{j-1,n})]$$

where $F_{j,n} = \frac{u_{j,n}^2}{2}$ and the *Jacobian matrix A* at the half intervals are calculated as

$$A_{j+\frac{1}{2},n} = \frac{u_{j,n} + u_{j+1,n}}{2} \quad \text{and} \quad A_{j-\frac{1}{2},n} = \frac{u_{j,n} + u_{j-1,n}}{2}$$

along with the stability requirement of

$$\left|\frac{\Delta t}{\Delta x} u_{\max}\right| \leq 1.$$

5 Results

Statement of the problem. Here, consider the following initial and boundary conditions

$$\begin{cases} u(x,0) = \sin(\pi x), & 0 < x < 1 \\ u(0,t) = u(1,t) = 0, & t > 0 \end{cases} \#(5.1.1)$$

The Hopf-Cole transformation of (5.1.1.) is then

$$\begin{cases} \theta(x,0) = \exp(-(2\pi\epsilon)^{-1}[1-\cos(\pi x)]), & 0 < x < 1 \\ \theta_x(0,t) = \theta_x(1,t) = 0, & t > 0. \end{cases} \#(5.1.2)$$

5.1.1 Viscid

The exact solution of (3.1.5) is then given as [6]

$$u(x,t) = 2\pi\epsilon \frac{\sum_{n=1}^{\infty} a_n e^{-n^2\pi^2\epsilon t} n\sin(n\pi x)}{a_0 + \sum_{n=1}^{\infty} a_n e^{-n^2\pi^2\epsilon t}\cos(n\pi x)} \#(5.1.3a)$$

where

$$a_0 = \int_0^1 e^{-\frac{1-\cos(\pi x)}{2\pi\epsilon}} dx \#(5.1.3b)$$

and

$$a_n = 2\int_0^1 e^{-\frac{1-\cos(\pi x)}{2\pi\epsilon}} \cos(n\pi x)\, dx, \qquad n \geq 1 \#(5.1.3c)$$

Note that the integrals (5.1.3b) and (5.1.3c) can be expressed in terms of Bessel functions; hence equation (5.1.3a) can be computed as

$$u(x,t) = 4\pi\epsilon \frac{\sum_{n=1}^{\infty} e^{-n^2\pi^2\epsilon t} n I_n(\frac{u_0}{2\pi v})\sin(n\pi x)}{I_0(\frac{u_0}{2\pi v}) + 2\sum_{n=1}^{\infty} e^{-n^2\pi^2\epsilon t} I_n(\frac{u_0}{2\pi v})\cos(n\pi x)} \#(5.1.4)$$

where I_0 and I_n are modified Bessel functions of the first kind [1]. The following is a statement from [3], cautioning against the usage of Bessel functions:

> *"This analytical solution is numerically untractable at small* t $(0 \leq t \leq 2\pi)$ *and* v *as* $I_n(z)$ *with z going to infinity behaves asymptotically as* $e^z(2\pi z)^{-\frac{1}{2}}$ *independent of n."*

In figure 4a, comparisons are made among the solutions obtained from the analytical solution, the FTCS scheme and the Crank-Nicolson scheme. The parameters involved were $\Delta t = 0.00001$,

$\Delta x = \frac{1}{80}$ and $\epsilon = 1$. Some of the solutions are shown in the table and both schemes produce agreeing results.

Figure 4a: Comparison of solutions from at $\epsilon = 1, \Delta x = \frac{1}{80}$ and $\Delta t = 0.00001$

t	x	Exact	FTCS	Crank-Nicolson
$\mathbf{0.1}$	0.1	0.1095382	0.1095289	0.1095241
	0.3	0.2918964	0.2918722	0.2918587
	0.5	0.3715775	0.3715477	0.3715292

Furthermore, the accuracy of both the FTCS and Crank-Nicolson are computed using equations (4.1.2a-b) and shown in Figure 4b. The two numerical schemes return errors of small magnitudes.

Figure 4b: Accuracy comparison at $\Delta t = 0.00001$,$\Delta x = \frac{1}{80}$ and $\epsilon = 1$

		FTCS		Crank − Nicolson	
t	N	$\|\|error\|\|_2$	$\|\|error\|\|_\infty$	$\|\|error\|\|_2$	$\|\|error\|\|_\infty$
$\mathbf{0.1}$	**80**	$2.10097e-05$	$2.973187e-05$	$3.420002e-05$	$4.838738e-05$

Next, the time step intervals are increased to $\Delta t = 0.005$ to illustrate the importance of stability. The rest of the parameters remain the same. Indeed, it can be observed from figures 5(a,b) that both FTCS and Crank-Nicolson schemes suffer in accuracy. More importantly, as the FTCS scheme is a conditionally stable scheme, it is no longer stable with the new and larger time step interval. Thus, the approximations are inaccurate. On the other hand, one can notice the Crank-Nicolson having increase in the magnitude of error, this can be expected for the truncation errors. Nonetheless, its approximations remain stable despite the larger time step due to being an unconditionally stable numerical scheme.

Figure 5a: Comparison of solutions from at $\epsilon = 1, \Delta x = \frac{1}{80}$ and $\Delta t = 0.005$

t	x	Exact	FTCS	Crank-Nicolson
$\mathbf{0.1}$	0.1	0.1095382	4.337343	0.1094927
	0.3	0.2918964	−138.956	0.2917844
	0.5	0.3715775	51.43078	0.3714543

Figure 5b: Accuracy comparison at $\Delta t = 0.005$,$\Delta x = \frac{1}{80}$ and $\epsilon = 1$

	FTCS	Crank − Nicolson

t	N	$\|\|error\|\|_2$	$\|\|error\|\|_\infty$	$\|\|error\|\|_2$	$\|\|error\|\|_\infty$
0.1	**80**	945.0245	6416.754	$8.72524e-05$	$1.259611e-04$

5.1.2 Inviscid

Here, consider the initial condition from (5.1.1) again with a slight modification

$$u(x,0) = \sin(\pi x), \qquad x \in [0,2]. \#(5.1.5)$$

The implicit solution for (3.2.1) can be obtained as

$$u(x,t) = \sin(x - ut)$$

where the characteristic lines projected onto the $(x - t)$ plane are described by

$$x(t) = x(0) + \sin(x)t.$$

The characteristic lines are shown in figure 6 where intersections of the lines can be observed. The breaking time (3.2.8) is

$$\tau = -\frac{1}{-1} = 1$$

Due to the symmetrical nature of the sine curve, $u_L = -u_R$ and the shock propagation speed can then be deduced as $s = 0$. Thus, there is no propagation of shock.

Figure 5: Characteristic lines of the $(5.1.5)$ projected onto the $(x - t)$ plane

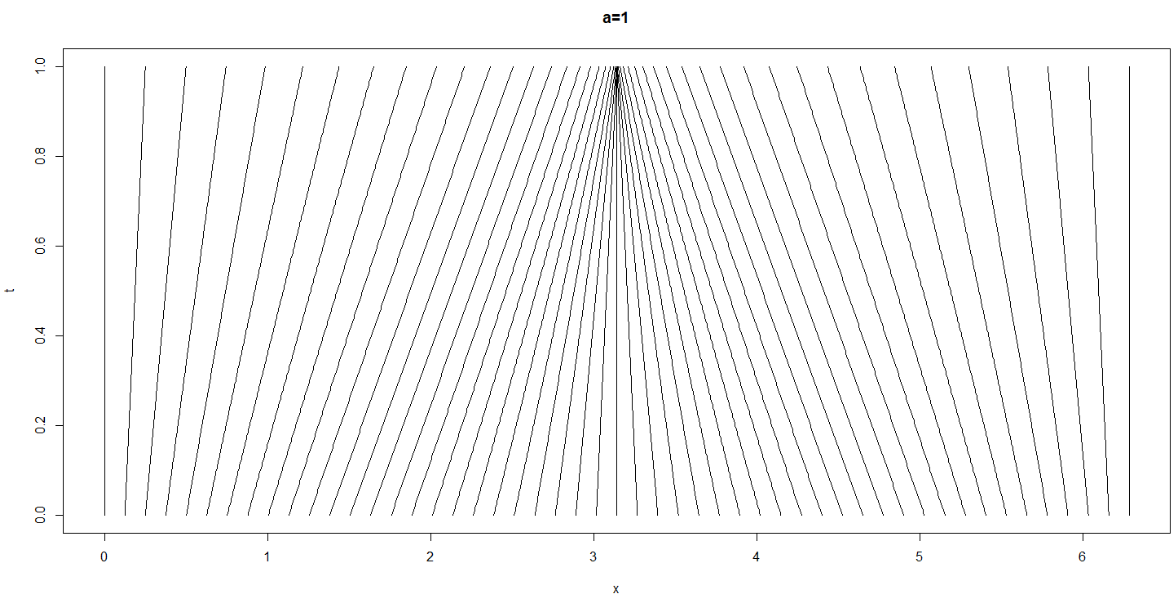

From figure 7, one could observe the sine waveforms for both Lax and Lax-Wendroff solutions become sharper as t increases, indicating a distortion phenomenon. Furthermore as time t increase, the Lax-Wendroff solutions begin to fluctuate sharply as the wave forms steepen. This signals that shock waves have occur. The parameters used $\Delta t = 0.0001$, $\Delta x = \frac{1}{300}$ and time considered were $T = \{0.01, 0.1, 0.5, 1\}$.

Figure 6: Simulations with different t values using Lax and Lax-Wendroff methods

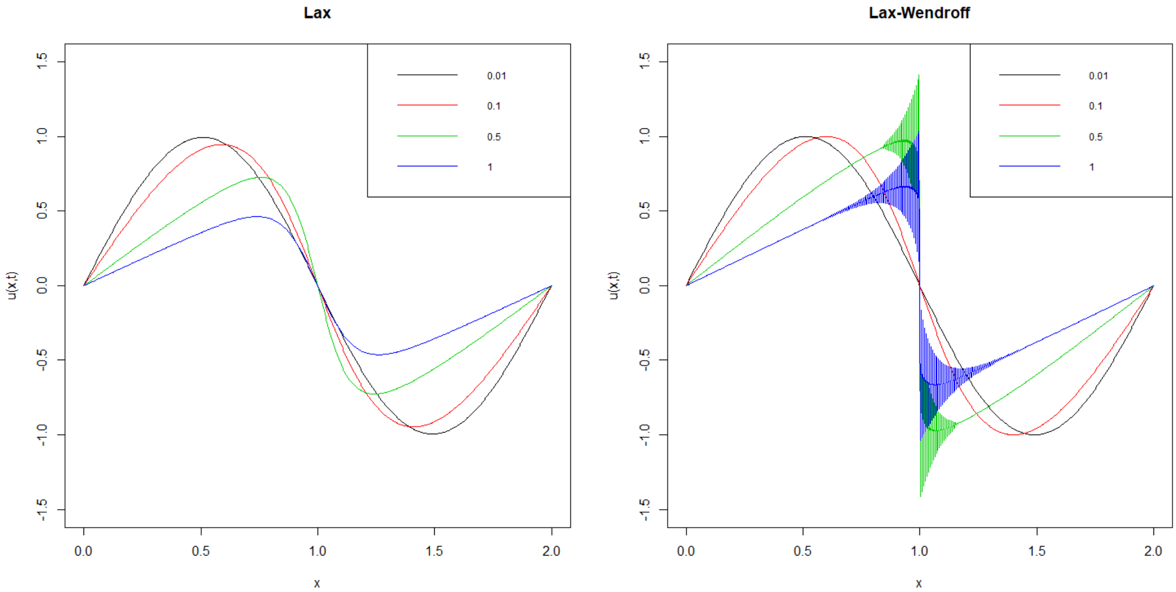

Unfortunately, as the analytical solution was not found, no accuracy assessment could be made about the two schemes.

6 Vanishing viscosity

In this section, the effects of viscosity will be examined again. In particular, recall when determining unique weak solutions, much of the motivation behind the inviscid Burgers' equation originates from physical behaviors, i.e. conservation laws. Another less physically biased method is the vanishing viscosity approach, i.e. in equation (1.1) as $\epsilon \to 0$, the "true" solution of the inviscid equation will be revealed.

Returning back to the problem from section 5, some snapshots of the Burgers equation plotted using different viscosity values in figures 8 and 9. As ϵ decreases, it seems that the waveforms are being split into two, where one side is moving upwards while the other moves downwards. Indeed, this illustrates the vanishing viscosity concept.

Figure 8: Exact solutions for $\epsilon = 0.80$ (left) & $\epsilon = 0.35$ (right) with $\Delta x = 0.005$ & $\Delta t = 0.005$

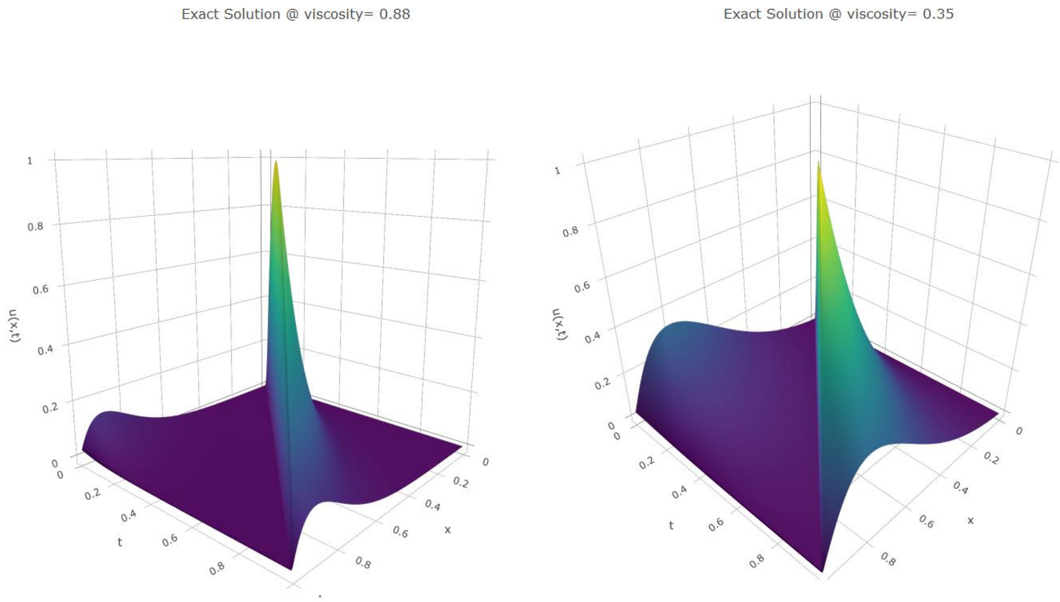

Figure 9: Exact solutions for $\epsilon = 0.01$ (left) & Lax-Wendroff solutions for $\epsilon = 0$with $\Delta x = 0.005$ & $\Delta t = 0.005$

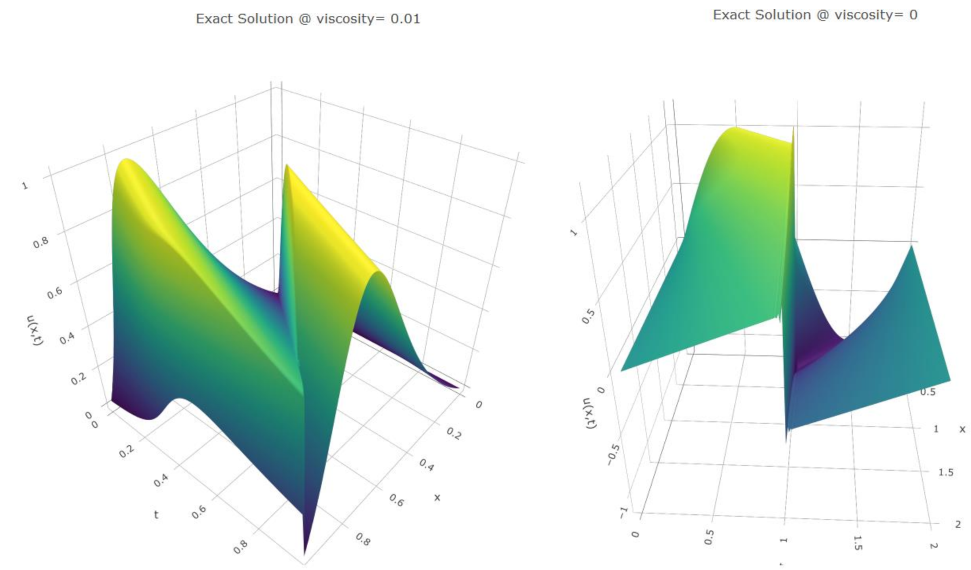

Figure 10: Illustration of the effects large viscosity, $\epsilon = 10$ with $\Delta x = 0.005$ & $\Delta t = 0.005$

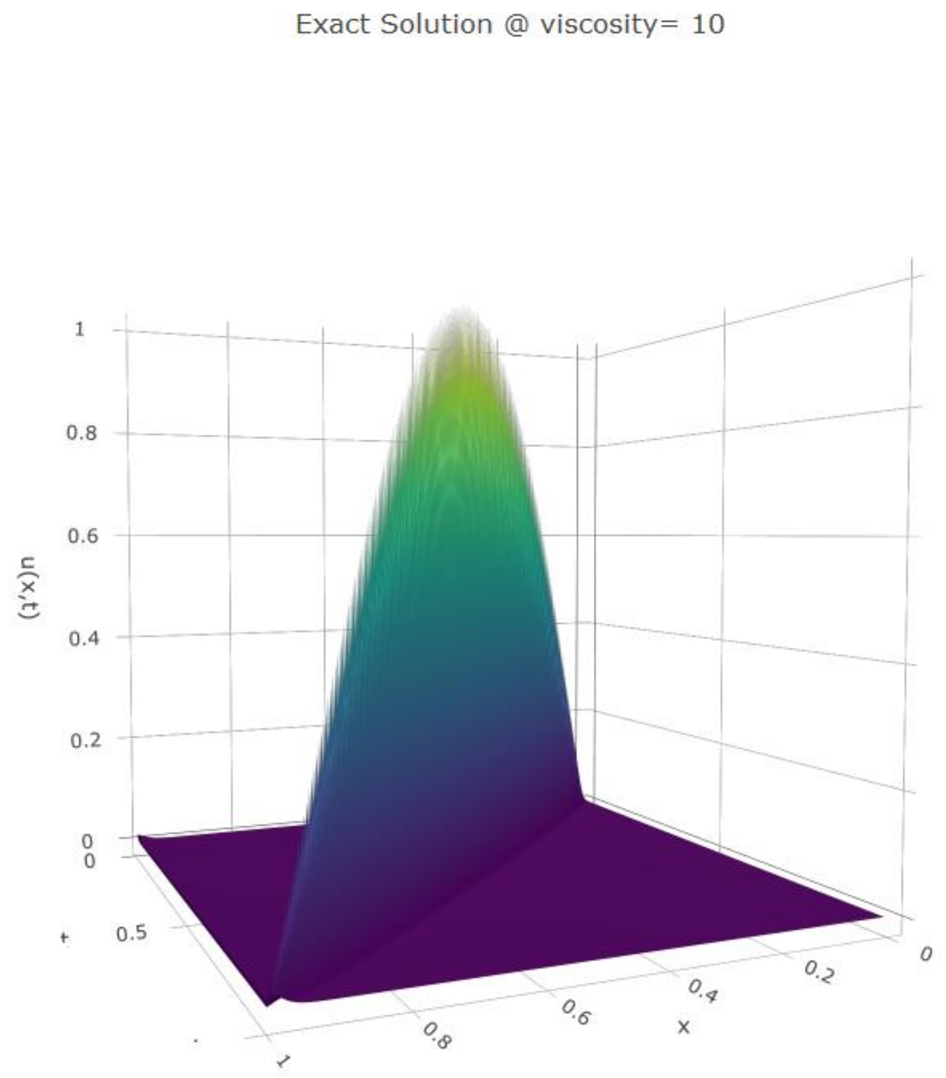

Lastly, an illustration of the exact solutions (5.1.4) with $\epsilon = 10$ is shown in figure 10 where one can observe the waveforms have been flatted out by the diffusion, with a single dissipative "flat" hump remaining.

References:

[1] Abramowitz, M. and Stegun, I. (1972). Handbook of mathematical functions with formulas, graphs, and mathematical tables. Washington, D.C.: U.S. Dept. of Commerce, National Bureau of Standards.

[2] Anderson, Dale A. (Dale Arden), Tannehill, J.C. & Pletcher, R.H. 1984, Computational fluid mechanics and heat transfer, Hemisphere, London;Washington;.

[3] Basdevant, C., Deville, M., Haldenwang, P., Lacroix, J., Ouazzani, J., Peyret, R., Orlandi, P. and Patera, A. (1986). Spectral and finite difference solutions of the Burgers equation. Computers & Fluids, 14(1), pp.23-41.

[4] BENTON, E.R. & PLATZMAN, G.W. 1972, "A TABLE OF SOLUTIONS OF THE ONE-DIMENSIONAL BURGERS EQUATION", Quarterly of Applied Mathematics, vol. 30, no. 2, pp. 195-212.

[5] Bonkile, M.P., Awasthi, A., Lakshmi, C., Mukundan, V. & Aswin, V.S. 2018, "A systematic literature review of Burgers' equation with recent advances", Pramana, vol. 90, no. 6, pp. 1-21.

[6] Cole, J. (1951). On a quasi-linear parabolic equation occurring in aerodynamics. Quarterly of Applied Mathematics, 9(3), pp.225-236.

[7] Debnath, L. (2012). Nonlinear Partial Differential Equations for Scientists and Engineers. 3rd ed. Birkhäuser.

[8] Evans, L.C., 1949 2010, Partial differential equations, 2nd edn, American Mathematical Society, Providence, R.I.

[9] Fletcher, C.A.J. 1988, Computational techniques for fluid dynamics: Vol.1, Fundamental and general techniques, Spinger-Verlag, Berlin;London;.

[10] Gladwell, I. & Wait, R. 1979, A survey of numerical methods for partial differential equations, Clarendon Press, Oxford.

[11] GomezS.,C.A.:AnoteontheexactsolutionforthefractionalBurgersequation.Int.J.PureAppl.Math.93(2),229–232 (2014)

[12] INAN, B. & BAHADIR, A.R. 2013, "Numerical solution of the one-dimensional Burgers' equation: Implicit and fully implicit exponential finite difference methods", Pramana, vol. 81, no. 4, pp. 547-556.

[13] Iserles, A. 1996, First course in numerical analysis of differential equations, Cambridge University Press, Cambridge

[14] Kadalbajoo, M.K. & Awasthi, A. 2006, "A numerical method based on Crank-Nicolson scheme for Burgers' equation", Applied Mathematics and Computation, vol. 182, no. 2, pp. 1430-1442.

[15] Kreiss, H.(. & Lorenz, J. 1989, Initial-boundary value problems and the Navier-Stokes equations, Academic Press, Boston.

[16] Kutluay, S., Bahadir, A.R. & Özdeş, A. 1999, "Numerical solution of one-dimensional Burgers equation: explicit and exact-explicit finite difference methods", Journal of Computational and Applied Mathematics, vol. 103, no. 2, pp. 251-261.

[17] Lax, P.D. & Society for Industrial and Applied Mathematics 1973, Hyperbolic systems of conservation laws and the mathematical theory of shock waves, Society for Industrial and Applied Mathematics, Philadelphia.

[18] LeVeque, R. (1992). Numerical Methods for Conservation Laws. Birkhäuser Basel.
[19] Momani,S.:Non-perturbativeanalyticalsolutionsofthespace-andtime-fractionalBurgersequations.ChaosSolitons Fractals 28(4), 930–937 (2006)
[20] Smith, G.D. 1985, Numerical solution of partial differential equations: finite difference methods, 3rd edn, Clarendon Press, Oxford.
[21] Wazwaz, A. (2007). Multiple-front solutions for the Burgers equation and the coupled Burgers equations. Applied Mathematics and Computation, 190(2), pp.1198-1206.
[22] Wazzan, L. 2009, "A modified tanh–coth method for solving the KdV and the KdV–Burgers' equations", *Communications in Nonlinear Science and Numerical Simulation,* vol. 14, no. 2, pp. 443-450.